

## Neutron capture cross section of manganese

J. B. Garg

State University of New York at Albany, Albany, New York 12222

R. L. Macklin and J. Halperin

Oak Ridge National Laboratory, Oak Ridge, Tennessee 37830

(Received 14 November 1977)

Total neutron capture cross section measurements have been carried out for  $^{55}\text{Mn}$  ( $I = 5/2$ ) over the energy interval of 2.5–600 keV. Using time-of-flight techniques and a nonhydrogenous liquid scintillator detector system, resonance energies and capture area were determined for some 143 resonances to 112 keV neutron energy. Values of radiation widths ( $\Gamma_\gamma$ ) were evaluated for broad  $l = 0$  resonances using published total cross section data. Although values of  $\Gamma_\gamma$  vary widely for individual resonances, mean values of  $\langle\Gamma_\gamma\rangle_{l=0} = 750 \pm 150$  and  $\langle\Gamma_\gamma\rangle_{l=1} = 400 \pm 100$  meV were determined. The correlation between  $\Gamma_\gamma$  and  $\Gamma_n^0$  (for  $s$ -wave resonances) was found to give  $\rho = 0.64 \pm 0.14$  which is statistically significant at the 99.9% confidence level.

[NUCLEAR REACTIONS  $^{55}\text{Mn}(n, \gamma)^{56}\text{Mn}$ ,  $E = 3.0\text{--}600$  keV; measured  $\sigma_{n,\gamma}(E)$ , deduced the resonance parameters;  $E_0$ ,  $\Gamma_n$ ,  $(\Gamma_\gamma)_l$ ,  $S_l$ ,  $\langle D \rangle_{l=0}$ ,  $\langle D \rangle_{l=1}$ ,  $\rho(\Gamma_n^0, \Gamma_\gamma)$ .]

## INTRODUCTION

Precise information on the neutron capture cross sections in manganese ( $^{55}\text{Mn}$ ) is valuable for reactor design in view of its use as an alloy in structural material. This information contributes to our understanding of neutron interactions with nuclei through the measurements of resonance parameters by characterizing individual resonances ( $E_0, \Gamma_n, \Gamma_\gamma, J^\pi, l$ ) as well as their average properties and fluctuations about their mean values. An examination of the correlation between resonance neutron and radiation widths ( $\Gamma_n$  and  $\Gamma_\gamma$ ) provides evidence for model interpretations. The investigation of capture cross sections complements total cross section measurements which provide reliable information for neutron widths. Although several measurements of total cross sections in manganese have been reported in the past few years,<sup>1-3</sup> only one measurement<sup>4</sup> of capture cross sections for this nucleus has been reported to date. In view of the capture measurement's greater sensitivity for resonances with very small  $\Gamma_n$ 's this technique is also useful in determining parameters of resonances of higher orbital angular momenta  $l=1$  and  $l=2$ , provided that proper account is taken of the additional weak  $s$ -wave levels. An estimate of the number of weak  $s$ -wave levels can be made by investigating the neutron width distribution. Finally the measurements of precise capture cross sections in the 10–100 keV region are of some importance in understanding the nucleosynthesis of elements in stellar interiors which takes place by successive capture of neutrons.

## EXPERIMENTAL DETAILS

The cross sections were measured at the 40 m station of the Oak Ridge Electron Linear Accelerator (ORELA). The experimental arrangements and equipment have been described in earlier publications,<sup>5,6</sup> and only a brief summary relevant to the present measurements is given here.

The sample of natural manganese weighing 7.765 g in the form of a rectangular plate 2.62 cm  $\times$  2.56 cm  $\times$  0.2 cm ( $n = 0.0127$  atoms/b) is centrally placed between a pair of total energy  $\gamma$ -ray detectors. A calculated pulse-height weighting technique provides an average detector response for capture  $\gamma$  rays proportional to the total energy of the capture event. These nonhydrogenous fluorocarbon scintillators yield low backgrounds with a time resolution better than 2 nsec and a  $\gamma$ -cascade efficiency of about 15% per neutron captured. The beam burst width used in these experiments was 5 ns, giving a nominal time resolution at the highest energy of about 0.1 ns/m. This is a factor of about 4 better than the best total cross section measurements<sup>1-3</sup> made to date for this nucleus, and very much better than the only other capture measurements.<sup>4</sup>

## ANALYSIS

The capture cross section of neutrons by a nucleus due to a resonance is described by the Breit-Wigner single level formula,

$$\sigma_{n,\gamma} = \pi \lambda^2 \omega_0^2 \frac{\Gamma_n \Gamma_\gamma}{(E - E_0)^2 + (\Gamma/2)^2},$$

where  $g_j$  is the statistical weight factor,  $\Gamma_n$  is the value of the neutron width at  $E_0$  and  $\Gamma_\gamma$  and  $\Gamma$  are the radiation and total widths, respectively.  $E_0$  is the resonance energy and  $\lambda$  corresponds to the neutron wavelength divided by  $2\pi$  at energy  $E$ . This expression is valid for an isolated resonance but does not take into account contributions to  $\sigma_{n,\gamma}$  from other neighboring resonances.

Analyses of individual resonances (in terms of the single level formula) were carried out with a generalized least-squares-fit program (LSFIT<sup>8</sup>). The program takes into account Doppler broadening, instrumental resolution, resonance self-protection and provides a background term having  $1/\nu$  dependence. The program also handles multiple scattering in the sample, following neutrons to the fourth interaction. A comparison of the adequacy of the multiple scattering treatment here with Monte Carlo calculations showed no appreciable differences up to multiple scattering contributions of  $\sim 50\%$  of the observed capture yield. The program also has provision for adjusting an asymmetric tail to the primarily Gaussian shape of the experimental resolution function. If the neutron width  $\Gamma_n$  is independently known or is appreciably greater than the resolution, the radiative width will be uniquely evaluated. If the total width is less than  $\sim \frac{1}{4}$  of the resolution, either  $\Gamma_n$  or  $\Gamma_\gamma$  must be fixed in the analysis to achieve convergence.

The area fit evaluates the thin sample capture area ( $A_\gamma = 2\pi^2 \lambda_0^2 g \Gamma_n \Gamma_\gamma / \Gamma$ ) and the kernel,  $g \Gamma_n \Gamma_\gamma / \Gamma$  is listed in Table I. In the limit where  $\Gamma_\gamma \gg \Gamma_n$  the kernel approaches  $g \Gamma_n$ , and conversely for  $\Gamma_n \gg \Gamma_\gamma$  (which tends to be the case at higher energies) the kernel approaches  $g \Gamma_\gamma$ .

An important consideration in the determination of  $\Gamma_\gamma$  is the sensitivity of the capture detector to scattered neutrons. This provides a correction to the observed values of  $\Gamma_\gamma$  obtained in the least-squares fit. This correction has been applied in the thin sample approximation as

$$\Gamma_\gamma = \Gamma_{\gamma(\text{obs})} - k \Gamma_n.$$

It was first formulated and evaluated using the <sup>7</sup>Li resonance near 250 keV for which the ratio of  $\Gamma_\gamma$  to  $\Gamma_n$  was known to be extremely small.<sup>6</sup>

To obtain detailed information on the energy dependence of the scattered neutron sensitivity of our apparatus, we have used off-resonance scattering from samples of <sup>12</sup>C and <sup>208</sup>Pb (see Ref. 7 for data and discussion). As the energy loss on elastic scattering varies inversely as the mass of the compound nucleus, the structure is best shown with the <sup>208</sup>Pb sample. Features evident in the data, are attributed to scattered neutron capture in the fluorine nuclei of the C<sub>6</sub>F<sub>6</sub> scintillation detector, aluminum in the detector

mounting, and silicon in the quartz scintillator cells and light pipes. Some of the residual, smoothly energy-dependent sensitivity may be attributed to the boron found in the pyrex phototube faces. The <sup>208</sup>Pb off-resonance yield<sup>7</sup> has been parametrized so that the sensitivity for lighter nuclei such as manganese can be computed including the effects of greater energy loss on scattering.

The correction ranges from about  $k = 10^{-3} - 10^{-4}$  over the energy span of this experiment and is considered good to 35% or less for such a thin sample. The 35% uncertainty in the correction noticeably increases the error in  $\Gamma_\gamma$  over the statistical uncertainty only for the broad  $l = 0$  resonances.

The data in terms of effective cross section versus energy are illustrated in Figs. 1 and 2. The limitations due to resolution are apparent especially at energies above 100 keV and therefore analyses of individual resonances have only been carried out to 112 keV.

The analysis of very broad resonances requires appreciable corrections for multiple scattering and self-shielding which are incorporated only approximately in the LSFIT analysis. We have made use of a Monte-Carlo program TACASI<sup>9</sup> for such broad resonances. A comparison of an analysis of the *s*-wave doublet at 7102 and 8815 eV by LSFIT and TACASI illustrates the degree to which  $\Gamma_\gamma$  is underestimated with the former as multiple scattering exceeds the 50% level. For the 8815 ( $J = 3$ ) resonance, the analysis using the least-squares-fitting program gave  $\Gamma_n = 370 \pm 11$  eV and  $\Gamma_\gamma = 1.20 \pm 0.04$  eV with a multiple scattering factor of 1.64. See Fig. 3. A series of Monte Carlo calculations in which  $\Gamma_n$  was varied yielded a best value of  $\Gamma_\gamma = 1.16 \pm 0.05$  eV. Although the degree of multiple scattering varied with  $\Gamma_n$ , values of  $\Gamma_\gamma$  were insensitive to the variation. For the 7102 ( $J = 2$ ) resonance, the least-squares analysis yielded  $\Gamma_n = 398 \pm 10$  eV and  $\Gamma_\gamma = 1.41 \pm 0.04$  eV with a multiple scattering factor of 1.72. See Fig. 4. Figure 5 shows the TACASI fits to both of these resonances. Fixing  $g \Gamma_n$  at a value of 30% greater only increased  $\Gamma_\gamma$  to 1.47 eV. A series of a Monte Carlo calculations in which  $\Gamma_n$  was varied yielded a value of  $\Gamma_\gamma = 1.40 \pm 0.05$  eV. Within the accuracy of the current analysis the least-squares fitting of the resonance would appear to be in agreement with the Monte Carlo calculation up to multiple scattering corrections as high as 1.7. Both values of  $\Gamma_\gamma$  require correction for the resonance scattered neutron sensitivity factor  $k$  described earlier. Table I summarizes the parameters for all resonances up to 112 keV as determined in the least-squares analysis including the neutron sensitivity correction for

TABLE I. Parameters of all resonances up to 112 keV for  $^{55}\text{Mn}$  analyzed by the LSFRIT program. The asterisk indicates the resonances which are assigned as s wave.  $g\Gamma_n\Gamma_\gamma/\Gamma$  are proportional to the observed area for the resonances with  $\Gamma_\gamma$  assumed or calculated. The values of effective  $\Gamma_\gamma$ 's after correction for the neutron scattering effect are given in column 6.

$E_0$ (keV)	$\frac{g\Gamma_n(\Gamma_\gamma+k\Gamma_n)}{\Gamma}$ (meV)		$g\Gamma_n$ (eV)	$\Gamma_\gamma+k\Gamma_n$ (meV)	$k$ ( $10^{-3}$ )	$(\Gamma_\gamma)$ (meV)	$g$
4.000	0.6 ±	0.1	$0.62 \times 10^{-3} \pm 0.68 \times 10^{-4}$	300			0.5
4.302	1.9 ±	0.1	$0.192 \times 10^{-2} \pm 0.12 \times 10^{-3}$	300			0.5
4.939	111.0 ±	2.8	0.466 ± 0.015	291.5 ± 12.5		291	0.5
6.330	65.2 ±	1.7	0.116 ± 0.005	300			0.5
6.960	3.6 ±	0.5	$0.365 \times 10^{-2} \pm 0.56 \times 10^{-3}$	300			0.5
*7.102	590 ±	10	166 ± 4	1424 ± 40	1.0	1026	0.417
*8.815	698.7 ±	22.0	216 ± 6	1200 ± 38	0.88	823	0.583
9.789	6.7 ±	0.5	$0.702 \times 10^{-2} \pm 0.54 \times 10^{-3}$	300			0.5
10.615	18.9 ±	0.7	0.0216 ± 0.89 × 10 <sup>-3</sup>	300			0.5
10.895	66.3 ±	1.9	0.12 ± 0.01	300			0.5
11.629	27.3 ±	0.9	0.0333 ± 0.14 × 10 <sup>-2</sup>	300			0.5
12.688	125.2 ±	7.7	0.557 ± 0.57 × 10 <sup>-1</sup>	323 ± 34.7	0.74	323	0.5
14.705	36.5 ±	1.0	0.048 ± 0.0017	300			0.5
14.948	81.6 ±	2.1	0.179 ± 0.01	300			0.5
16.167	105.1 ±	2.5	0.352 ± 0.028	300			0.5
17.725	28.4 ±	1.6	$0.35 \times 10^{-1} \pm 0.24 \times 10^{-2}$	300			0.5
*17.802	407.3 ±	6.9	6.4	750 ± 16	0.64	743	0.58
*17.990	207.2 ±	3.8	27	509 ± 10	0.64	467	0.41
18.812	124.0 ±	3.5	0.716 ± 0.12	300			0.50
19.127	5.5 ±	0.8	$0.567 \times 10^{-2} \pm 0.84 \times 10^{-3}$	300			0.50
20.225	81.8 ±	2.4	0.18 ± 0.011	300			0.50
20.488	1.9 ±	1.0	$0.19 \times 10^{-2} \pm 0.10 \times 10^{-2}$	300			0.50
20.824	73.8 ±	2.4	0.145 ± 0.93 × 10 <sup>-2</sup>	300			0.50
*20.852	750.0 ±	23.7	545	1295 ± 40	0.62	712	0.58
22.327	26.4 ±	1.4	$0.32 \times 10^{-1} \pm 0.2 \times 10^{-2}$	300			0.5
22.649	123.1 ±	3.0	0.70 ± 0.07	298.9 ± 8.8		299	0.5
*23.658	266.7 ±	10.2	168	652 ± 25	0.64	405	0.41
24.416	126.9 ±	3.2	1.0	290.8 ± 8.4	0.64	291	0.5
25.713	36.8 ±	2.0	$0.488 \times 10^{-1} \pm 0.36 \times 10^{-2}$	300			0.5
25.911	191.2 ±	46.2	1.65 ± 0.50	432.5 ± 135.5		432	0.5
*26.460	222 ±	8	55	546 ± 20	88	427	0.41
*26.983	812 ±	15	245	1404 ± 27	1.00	982	0.58
28.255	32.2 ±	2.1	0.041 ± 0.0035	300			0.5
28.741	123.8 ±	3.6	0.708 ± 0.12	300			0.5
*30.310	207 ±	28	6.2	443 ± 70	1.04	427	0.41
31.650	72 ±	4	0.11 ± 0.01	300			0.5
31.730	25 ±	4	0.028 ± 0.004	300			0.5
32.310	132 ±	5	0.389 ± 0.048	300			0.5
32.420	43 ±	4	0.060 ± 0.005	300			0.5
33.320	176 ±	13	4.2 ± 0.28	371 ± 31	1.04	364	0.5
34.877	42 ±	9	0.057 ± 0.012	400			0.5
35.248	71 ±	10	0.110 ± 0.025	400			0.5
*35.300	1618 ±	220	800	2795 ± 420	1.0	1416	0.58
*35.535	1106 ±	192	550	2705 ± 471	1.0	1363	0.41
36.545	169 ±	17	3.05 ± 0.28	361 ± 32	1.0	355	0.5
38.289	8 ±	4	0.001	400			0.5
38.392	42 ±	5	0.005	400			0.5
40.917	246 ±	14	4.2	518 ± 32	0.80	510	0.5
*40.920	623 ±	38	267	1076 ± 65	0.63	786	0.58
41.015	77 ±	9	0.124 ± 0.023	400			0.5
41.115	74 ±	7	0.116 ± 0.018	400			0.5
43.850	324 ±	12	5 ± 3	837 ± 26	0.60	830	0.5
44.045	176 ±	11	2.5 ± 2.0	400	0.60		0.5
45.340	116 ±	7	0.23 ± 0.03	400	0.60		0.5
*46.930	225 ±	10	8.4	561 ± 27	0.60	549	0.41
*47.635	86 ±	7	12	180 ± 16	0.62	168	0.58
48.345	118 ±	8	0.25 ± 0.03	400	0.68		0.5

TABLE I. (Continued)

$E_0$ (keV)	$\frac{g\Gamma_n(\Gamma_\gamma + k\Gamma_n)}{\Gamma}$ (meV)	$g\Gamma_n$ (eV)	$\Gamma_\gamma + k\Gamma_n$ (meV)	$k$ ( $10^{-3}$ )	$(\Gamma_\gamma)$ (meV)	$g$
51.125	184 ± 13	2.75 ± 2.20	400	0.72		0.5
52.450	150 ± 13	0.61 ± 0.18	400	0.72		0.5
52.820	8 ± 5	0.8 × 10 <sup>-2</sup> ± 0.5 × 10 <sup>-2</sup>	400			0.5
*53.390	235 ± 18	49	577 ± 43	0.64	500	0.41
54.187	236 ± 14	4	502 ± 30	0.62	497	0.5
*54.575	196 ± 14	12	516 ± 36	0.60	498	0.58
56.529	165 ± 9	1.06 ± 0.36	400			0.5
57.162	15 ± 11	0.017 ± 0.013	400			0.5
57.325	92 ± 15	0.17 ± 0.05	400			0.5
*57.380	486 ± 161	325	838 ± 280	0.5	558	0.58
*57.500	292 ± 125	216	697 ± 297	0.5	433	0.41
58.104	199 ± 11	0.5	660 ± 66	0.52	660	0.5
59.590	115 ± 13	0.27 ± 0.08	400			0.5
*59.815	445 ± 38	260	1075 ± 95	0.5	758	0.41
60.212	123 ± 12	0.32 ± 0.07	400			0.5
60.340	38 ± 11	0.04 ± 0.01	400			0.5
60.978	14 ± 7	0.015 ± 0.008	400			0.5
61.645	142 ± 11	0.5	395 ± 28		394	0.5
*61.980	203 ± 8	8.4	505 ± 22	0.43	480	0.41
*64.325	1157 ± 42	540	1998 ± 73	0.43	1598	0.58
64.600	42 ± 8	0.053 ± 0.012	400			0.5
*65.750	153 ± 11	21	377 ± 26	0.43	355	0.41
65.910	74 ± 8	0.12 ± 0.03	400			0.5
*66.612	357 ± 9	128	627 ± 35	0.43	532	0.58
67.420	87 ± 7	0.15 ± 0.02	400			0.5
*67.650	262 ± 12	25	647 ± 29	0.4	622	0.41
68.835	93 ± 11	0.17 ± 0.04	400			0.5
*69.550	240 ± 15	15	435 ± 43	0.4	425	0.58
*69.870	788 ± 80	358	1926 ± 196	0.4	1577	0.41
69.930	23 ± 15	0.027 ± 0.020	400			0.5
69.990	70 ± 17	0.11 ± 0.04	400	0.4		0.5
70.850	93 ± 11	0.17 ± 0.04	400	0.4		0.5
*71.190	280 ± 15	9.1 ± 0.7	575	0.4	568	0.41
*71.850	381 ± 18	20	662 ± 32	0.4	648	0.58
72.275	24 ± 8	0.03 ± 0.01	400			0.5
*72.962	208 ± 12	70	509 ± 209	0.4	494	0.41
74.000	58 ± 11	0.08 ± 0.02	400			0.5
*74.115	305 ± 13	6.0	641	0.4	635	0.41
*74.150	478 ± 76	510	825 ± 130	0.4	472	0.58
74.550	24 ± 11	0.028 ± 0.013	400			0.5
75.450	28 ± 11	0.03 ± 0.01	400			0.5
77.450	286 ± 53	7.4 ± 1.7	596 ± 117	0.4	590	0.5
*78.300	182 ± 14	21	475 ± 38	0.42	455	0.41
*79.342	205 ± 15	29	361 ± 28	0.43	338	0.58
81.320	145 ± 21	0.04 ± 0.17	400	0.44	798	0.5
*81.480	398 ± 57	165	975 ± 139	0.44		0.41
81.560	115 ± 22	0.18 ± 0.06	400	0.44		0.5
82.545	134 ± 15	0.22 ± 0.05	400	0.44		0.5
*83.525	318 ± 17	20	494 ± 22	0.45	479	0.58
83.900	122 ± 11	0.31 ± 0.07	400			0.5
84.175	96 ± 6	0.19 ± 0.03	400			0.5
84.800	156 ± 23	0.71 ± 0.50	400			0.5
84.980	396 ± 16	5	859 ± 38	0.46	855	0.5
*85.010	498 ± 26	360	785 ± 224		381	0.41
85.260	43 ± 15	0.05 ± 0.03	400			0.5
86.112	275 ± 50	1.91 ± 0.38	500	0.48		0.5
*86.290	193 ± 34	110	462 ± 81	0.49	369	0.58
86.490	244 ± 20	10.5 ± 0.8	500			0.5
86.570	38 ± 21	0.05 ± 0.03	400			0.5
87.175	82 ± 11	0.14 ± 0.03	400			0.5

TABLE I. (Continued)

$E_0$ (keV)	$\frac{g\Gamma_n(\Gamma_\gamma + k\Gamma_n)}{\Gamma}$ (meV)	$g\Gamma_n$ (eV)	$\Gamma_\gamma + k\Gamma_n$ (meV)	$k$ ( $10^{-3}$ )	$(\Gamma_\gamma)$ (meV)	$g$
88.750	267 ± 16	5.0	554 ± 30	0.6	539	0.5
89.737	190 ± 10	3.9	400			0.5
*91.400	466 ± 35	40	813 ± 62	0.6	772	0.58
*91.475	295 ± 35	25	728 ± 85	0.6	691	0.41
92.100	236 ± 5	4.37	500			0.5
93.750	128 ± 11	0.36	400			0.5
95.250	210 ± 10	3.75	450	0.65		0.5
*96.750	227 ± 26	100	557 ± 63	0.65	399	0.41
98.380	242 ± 20	8.6	500	0.65		0.5
98.825	64 ± 16	0.10	400	0.65		0.5
*98.975	892 ± 80	435	1541 ± 138	0.66	1046	0.58
99.250	93 ± 18	0.17	400			0.5
99.950	51 ± 15	0.07	400			0.5
100.48	96 ± 14	0.19	400			
*104.18	892 ± 24	54.1	1806 ± 50	0.64	1745	0.41
105.02	85 ± 20	2.0	180 ± 400		180	0.5
105.17	266 ± 22	8.9	549 ± 48	0.64	535	0.5
*105.37	1070 ± 154	916	2623 ± 375	0.64	1215	0.41
107.00	317 ± 18	10	655 ± 40	0.64	650	0.5
*107.90	835 ± 36	205	1996 ± 108	0.63	1681	0.41
108.94	362 ± 32	15	739 ± 67	0.62	720	0.58
109.65	103 ± 18	0.21	400			0.5
*110.20	218 ± 27	50	533 ± 66	0.60	460	0.41
110.60	70 ± 20	0.11	400			0.5
111.16	289 ± 22	5	614 ± 50	0.60	608	0.5
*111.35	2534 ± 243	2100	4553 ± 460	0.60	2380	0.58
111.57	179 ± 22	1.2	400	0.58		0.5
111.76	277 ± 22	5	588 ± 50	0.58	582	0.5

broad resonances.

#### DISCUSSION OF RESULTS

The broad resonance at about 35 keV has been reported by Garg<sup>1</sup> from a transmission measurement to be a doublet with  $\Gamma_n = (1820 \pm 200)$  eV for a  $J=3$  resonance and  $\Gamma_n = (730 \pm 70)$  eV for a  $J=2$  resonance. Using these values of  $g\Gamma_n$  in the analysis of the capture data, a relatively large value for  $\Gamma_\gamma$  (~3.8 eV) for the  $J=3$  resonance, and a negative value for the  $\Gamma_\gamma$  for the  $J=2$  resonance results. An analysis in which  $g\Gamma_n$  is varied is summarized in Table II. The results suggest that these two close  $l=0$  resonances of different spins have comparable neutron widths on the basis of nearly equal values for  $\Gamma_n$ . The comparable neutron widths of this doublet are also consistent, except for the  $J$  assignments, with the values obtained by Stephenson *et al.*<sup>11</sup> and Mughabghab *et al.*<sup>12</sup> from a reanalysis of the total cross section data of Garg *et al.*<sup>10</sup>

The analysis of the  $s$ -wave doublet near 57 keV is consistent with the neutron widths determined from the transmission measurement<sup>1</sup> but is not consistent with the results of Morgenstern *et al.*<sup>2</sup>

and Rohr *et al.*<sup>3</sup> There are other  $s$ -wave resonances whose neutron widths, determined by Garg<sup>1</sup> from total cross section measurements, do not provide good fits to the capture data. These resonances occur at energies of 71.80, 74.20, 91.90, 108.0 keV and are possibly doublets of different spins with smaller neutron widths as evaluated in the present experiment. Moreover we do not see in our capture data clear evidence for  $l=0$  resonances at 82.3 and 93.7 keV as reported by Garg.<sup>1</sup> We do observe narrow  $l=1$  resonances at these energies.

The transmission measurements are normally reliable for the assignment of  $l=0$  resonances due to their characteristic asymmetric shape. However, ambiguities may occur for weak  $l=0$  resonances, since these fail to show strong asymmetric shapes. Capture cross sections, on the other hand are quite sensitive for detecting narrow  $l=1$  and possibly  $l=2$  resonances. At neutron energies up to about 100 keV, the penetrabilities ( $P_l$ ) for higher angular momenta ( $l > 2$ ) are very small and hence, resonances with  $l > 2$  are too narrow to be observed. In the present measurements we have observed almost all of the  $l=0$  resonances as well as many narrower resonances. Many of these have not been observed in the transmission experi-

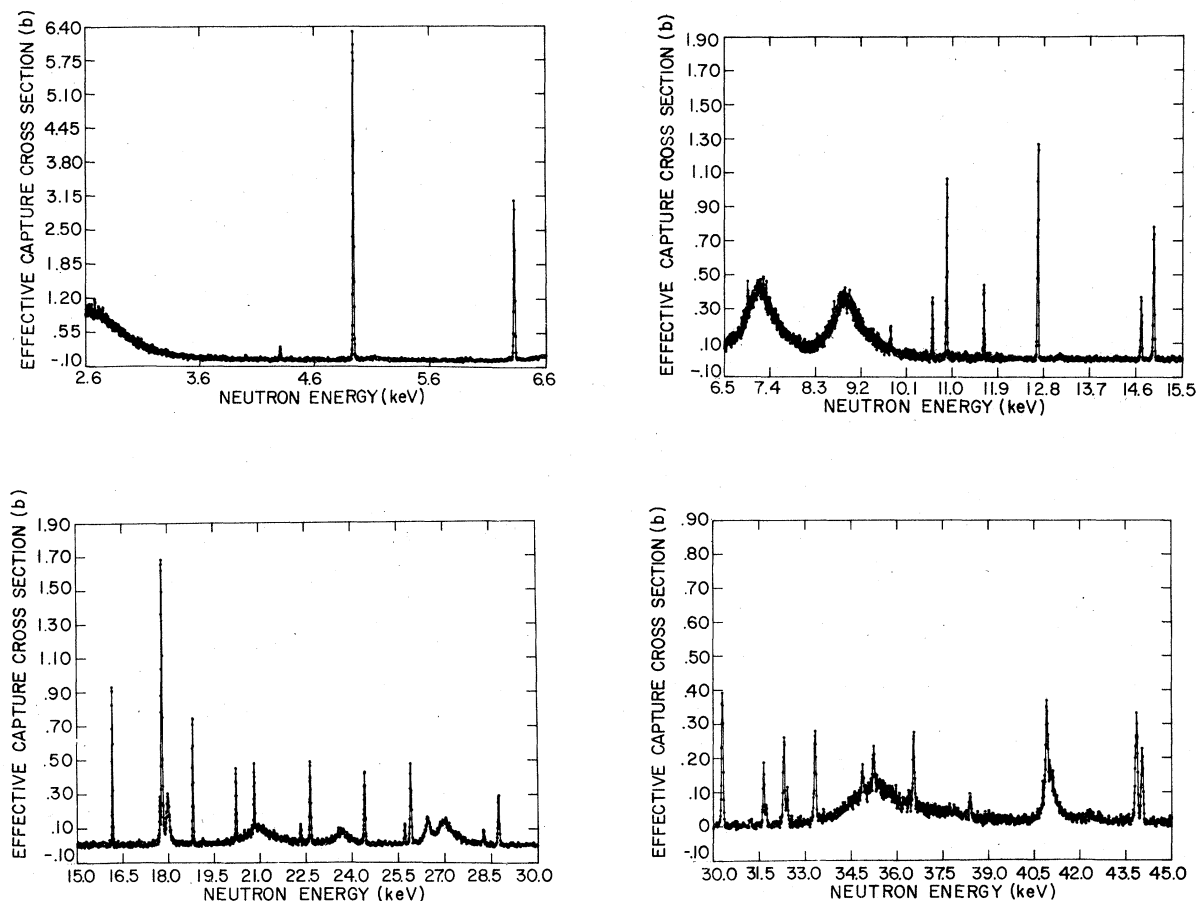


FIG. 1. Effective neutron capture cross sections for a thick metal sample of manganese.

ments<sup>10</sup> and are possibly  $l=1$  or  $l=2$  levels. Since the ground state of  $^{55}\text{Mn}$  is  $\frac{5}{2}^-$ , capture of  $s$ -wave neutrons would populate compound states with  $J^\pi = 2^-$  and  $3^-$ , whereas resonances with  $J^\pi = 1^+$ ,  $2^+$ ,  $3^+$ , and  $0^+$ ,  $1^-$ ,  $2^-$ ,  $3^-$ ,  $4^-$ ,  $5^-$  would be populated with  $l=1$  and  $l=2$  neutrons, respectively. Since  $l$  values rather than  $J$  values will ordinarily be evaluated from these measurements, only average values of the resonance parameters are obtained for different  $l$  values. For example the level density defined as

$$\rho_J(U) = \rho_0(U)(2J+1)\exp\left[-(J+\frac{1}{2})^2/2\sigma^2\right]$$

can be obtained for each  $l$  value. For  $\sigma = 3.5$  (Ref. 1) we obtain a ratio of mean spacing ( $D=1/\rho$ ) for  $l=0$  and  $l=1$  neutrons as  $D(l=0)/D(l=1) = 1.82$ .

The mean value of  $\langle D \rangle$  for  $s$ -wave resonances up to 100 keV neutron energy has been measured<sup>1</sup> as  $(1.96 \pm 0.20)$  keV. This value of  $\langle D \rangle$  is based on the assumption that all the resonances are  $s$  wave. On the basis of our capture measurements we feel that the resonances at energies of 6.33, 10.87, 25.89, 33.65, 36.40, 40.90, 43.80,

60.40, and 93.70 keV reported by Garg<sup>1</sup> as  $l=0$  are most likely  $p$  wave. Moreover the  $s$ -wave resonance he reports at 91.90 keV is most likely a close doublet with opposite spins. This is based on the large value of  $\Gamma_\gamma$  deduced when it is analyzed as a single resonance. This resonance has been analyzed as a doublet and the parameters are given in Table I. On the basis of the above corrections to the  $l$  assignments of resonances we obtain a revised value for the  $s$ -wave average spacing for Mn as  $\langle D \rangle_{l=0} = \frac{112}{50} = (2.24 \pm 0.25)$  keV. In the present capture measurements we have observed 100 non- $s$ -wave resonances from 4 keV to 112 keV giving a value for  $\langle D \rangle_{l=1} = (1.08 \pm 0.08)$  keV. This value of  $\langle D \rangle$  for  $p$ -wave resonances gives a ratio of  $D_{l=0}/D_{l=1} = (2.07 \pm 0.29)$ , which is somewhat larger than that given by the level density formula but is within the estimated uncertainties. It is, however, possible that some of these narrow resonances belong to  $l=2$  capture. In order to estimate the number of resonances which may belong to  $l=2$  we have investigated the reduced neutron width distribution of  $p$ -wave resonances.

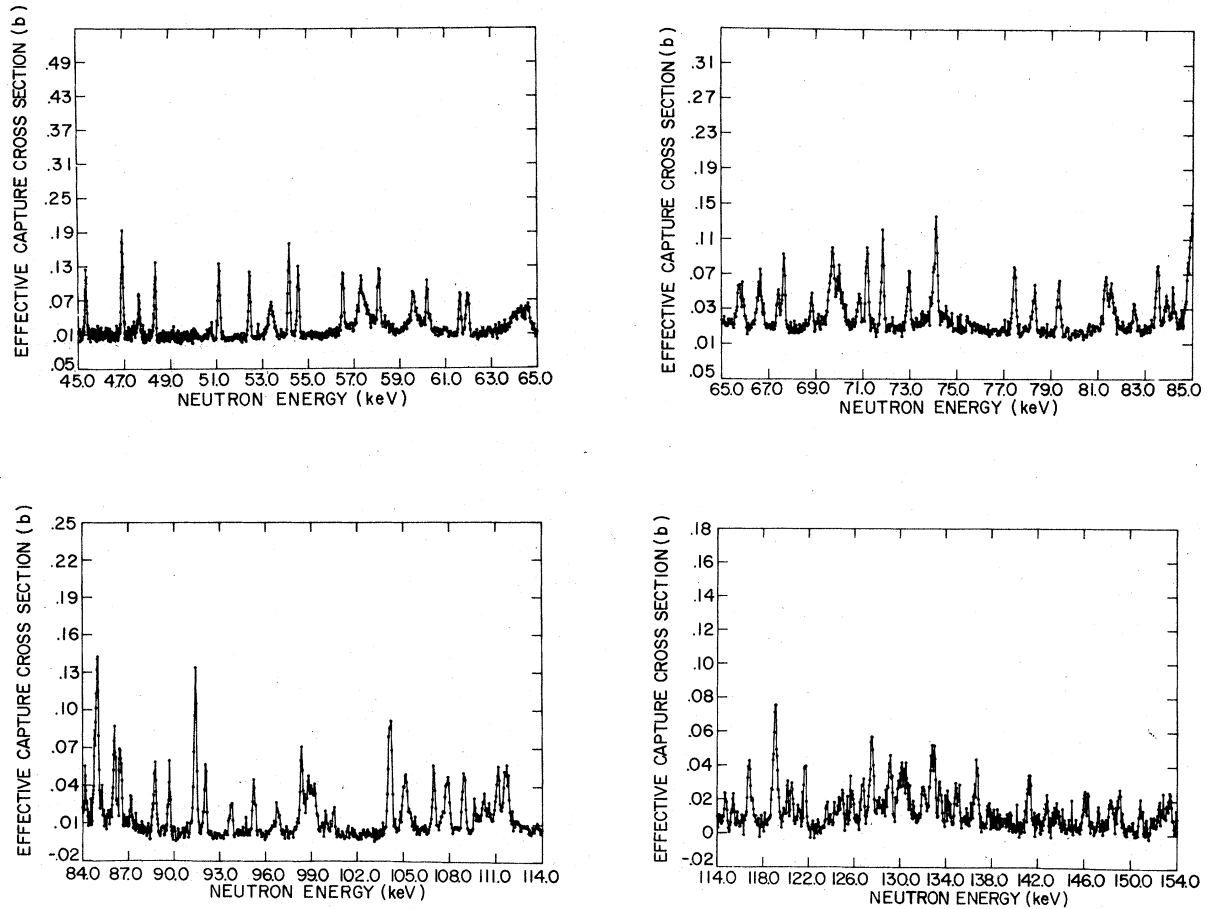


FIG. 2. Effective neutron capture cross sections for a thick metal sample of manganese.

Distribution of reduced neutron widths

The distribution of reduced neutron widths ( $\Gamma_n / \sqrt{E_n}$ ) for resonances of a single spin state about its mean value follows the Porter-Thomas distribution.<sup>13</sup> This distribution can be derived from

a consideration of the random distribution of the phases of the probability amplitudes  $\gamma_{\lambda n}$ 's which in turn are proportional to the square root of the neutron widths. The Porter-Thomas distribution is identical to a  $\chi^2$  distribution with one degree of freedom ( $\nu=1$ ),

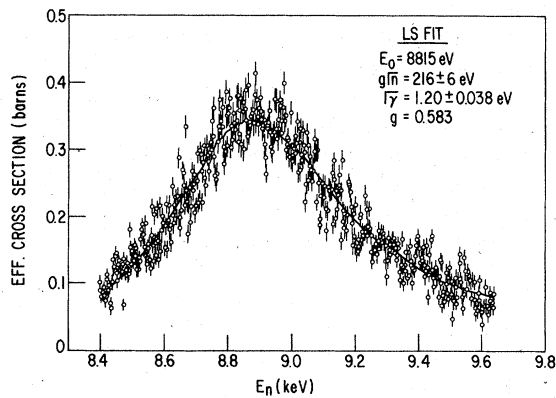


FIG. 3. The LSFIT analysis of a broad resonance at 8815 eV.

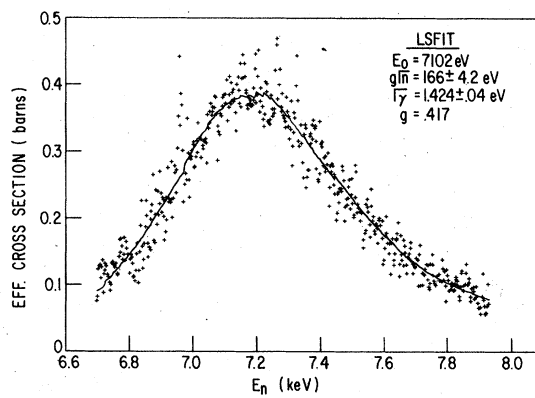


FIG. 4. The LSFIT analysis of a broad resonance at 7102 eV.

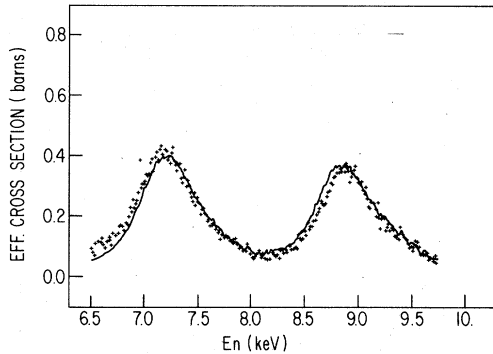


FIG. 5. A typical curve showing the analysis of TACASI fit for the doublet at 7102 and 8815 eV.

$$P(x)dx = \frac{(\frac{1}{2}\nu)(\frac{1}{2}\nu x)^{(\nu/2-1)} \exp(-\frac{1}{2}\nu x)}{\Gamma(\frac{1}{2}\nu)}$$

$$= \frac{\exp(-\frac{1}{2}x) dx}{(2\pi x)^{1/2}},$$

where  $P(x)$  is the probability of  $x$  lying between  $x$  and  $x+dx$  and

$$x = (\Gamma_n^i / \langle \Gamma_n^i \rangle).$$

Since  $s$ -wave neutron widths represent a single channel scattering process for an even-even target nucleus, the distribution of amplitudes, i.e., square roots of reduced neutron widths ( $y = x^{1/2}$ ), for the distribution may be written as

$$P(y)dy = (2/\pi)^{1/2} \exp(-y^2/2) dy.$$

This is of course the normal distribution with zero mean. The normalization constant will depend upon the number of resonances and the interval  $dy$ .

We have investigated the distribution of neutron reduced widths (in square-root form) about their mean values for both  $s$ - and  $p$ -wave resonances. Plots of these distributions along with the theoret-

tical distributions are shown in Figs. 6 and 7, respectively. The distribution for fifty  $s$ -wave resonances up to 112 keV neutron energy is in excellent agreement with the Porter-Thomas distribution; whereas the distribution for  $p$ -wave resonances shows an excess of about 18 small  $\Gamma_n^i$  over that expected from the Porter-Thomas distribution. Hence we are inclined to attribute this excess of small  $\Gamma_n^i$  to the presence of  $d$ -wave resonances in this series.

Since in the present measurements we have no way of separating  $p$ -wave levels according to spin, the distribution represents a mixture of 2 channel spins and 4 independent spins ( $J$ ) and thus the distribution in this case may differ from a  $\chi^2$  distribution with one degree of freedom. We have arbitrarily excluded very narrow resonances where  $(g\Gamma_n^i)^{1/2} < 0.06$  eV from the  $p$ -wave series and have assigned them as  $d$ -wave resonances. The elimination of these resonances gives better agreement with the Porter-Thomas distribution as is shown in Fig. 8.

#### Strength functions

The neutron strength function is a quantity of some interest in the investigation of the optical model potential, as well as contributing to the location of single particle or other states near the neutron binding energy which contributes to the strength. The strength function  $S_l$  for angular momentum  $l$  is defined as

$$S_l = \frac{1}{2l+1} \frac{\sum g\Gamma_n^i}{\Delta E},$$

where  $\Gamma_n^i$  is the neutron reduced width, and  $\Delta E$  is the energy interval over which  $\Gamma_n^i$  values are determined. Moreover,  $\Gamma_n^i$  can be expressed in terms of the penetrability factor  $P_l$  or  $V_l$  as  $\Gamma_n^i = \Gamma_n^0 / V_l$ , where  $\Gamma_n^0$  is the reduced neutron width for

TABLE II. The analysis of the unresolved doublet resonances at  $\sim 35$  keV by the LSFIT code using different values of  $g\Gamma_n$ . This table shows the dependence of  $\Gamma_\gamma$  on the assumed  $g\Gamma_n$ .

Case	$E_0$ (eV)	$g\Gamma_n \Gamma_\gamma / \Gamma$ (meV)	$g$	$g\Gamma_n$ (eV)	$\Gamma_\gamma$ (meV)	$(\Gamma_\gamma)_{\text{eff}}$ (meV)
I	35 300	3 258 $\pm$ 242	0.58	1 055	5 636 $\pm$ 420	3 800
II		2 440 $\pm$ 243	0.58	950	4 219 $\pm$ 421	2 581
III		2 027 $\pm$ 184	0.58	850	3 504 $\pm$ 320	2 038
IV		1 785 $\pm$ 192	0.58	850	3 085 $\pm$ 333	1 620
V		1 618 $\pm$ 220	0.58	800	2 795 $\pm$ 420	1 415
I	35 535	149 $\pm$ 97	0.41	300	362 $\pm$ 238	-370
II		465 $\pm$ 128	0.41	475	1 136 $\pm$ 313	-22
III		665 $\pm$ 160	0.41	500	1 625 $\pm$ 391	405
IV		747 $\pm$ 154	0.41	550	1 826 $\pm$ 377	485
V		1 106 $\pm$ 192	0.41	550	2 705 $\pm$ 471	1 365



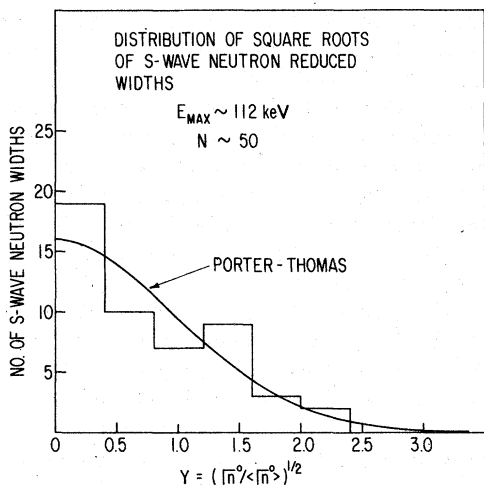


FIG. 6. Reduced neutron widths distribution for  $l=0$  resonances and the comparison with the Porter-Thomas distribution.

$l=0$  and  $V_l = P_l/(kR)$ ,  $P_0 = kR$ , and  $P_1 = (kR)^3/[1 + (kR)^2]$ . Thus the value of  $S_0$  is independent of the nuclear radius ( $R$ ), whereas the values of  $S_{l>0}$  will be dependent upon the value of the radius. We have evaluated the  $p$ -wave strength function from these measurements using the expression  $S_1 = \sum g \Gamma_n^1 / 3(E_f - E_i)$ . For a value of  $R = 4.5$  fm, we obtain  $S_1 = (0.36 \pm 0.05) \times 10^{-4}$  eV using all the levels listed in Table I as  $p$  wave and not marked with an asterisk. A value of  $S_1 = (0.35 \pm 0.05) \times 10^{-4}$  eV $^{-1/2}$  is obtained after eliminating the levels which we have taken to be  $d$  wave. As expected the value of  $S_1$  is quite insensitive to the elimination of these very narrow widths, but misassignments of weak  $s$ -wave levels to the  $p$ -wave distribution might increase the value of  $S_1$  significantly. However, the  $s$ -wave neutron width distribution (Fig.

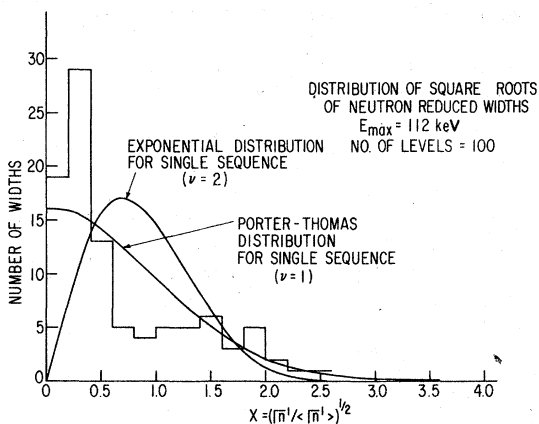


FIG. 7. Reduced neutron widths distribution (square-root form) for  $l > 0$  resonances and the comparison with the  $\chi^2$  distributions for  $\nu=1$  and  $\nu=2$ .

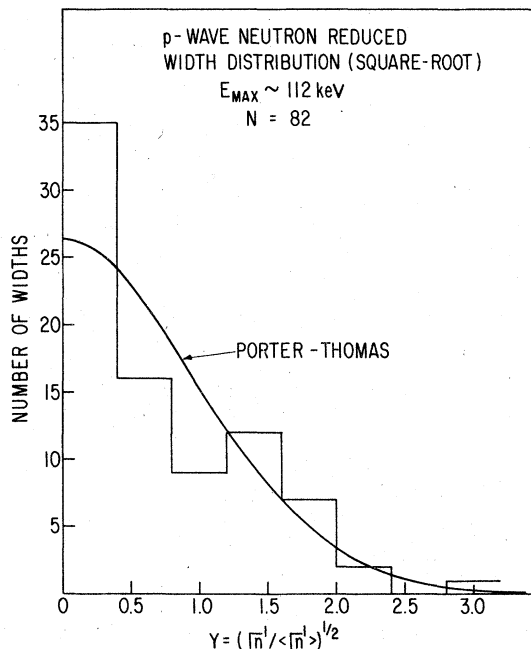


FIG. 8. Reduced neutron widths distribution (square-root form) for  $l=1$  resonances and the comparison with the Porter-Thomas distribution.

6) suggests that weak  $s$ -wave resonances have not been significantly missed.

A plot of the cumulative sum of  $g \Gamma_n^1$  vs  $E_n$  is shown in Fig. 9. The slope of the straight line passing through these points gives a measure of  $S_1$ . A straight line with a slope  $S_1 = (0.36_{-0.04}^{+0.05}) \times 10^{-4}$  eV $^{-1/2}$  may be fitted to the points below 20 keV and above 70 keV. However, a fit to points up to 50 keV gives a value of  $S_1 = (0.49_{-0.05}^{+0.09}) \times 10^{-4}$

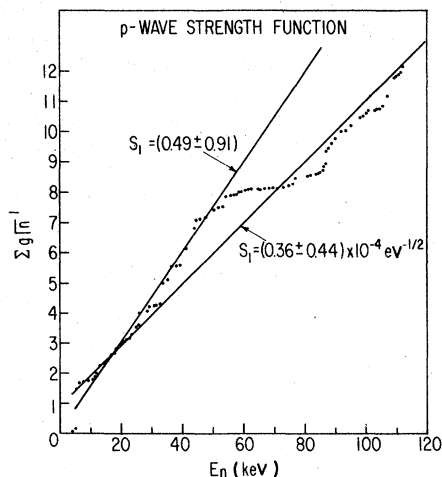


FIG. 9. A cumulative plot of  $\sum g \Gamma_n^1$  vs  $E_n$ . The slopes of the straight lines drawn through different neutron energy interval show the values of  $S_1$ .

$eV^{-1/2}$ . Although the discrepancy in the two values of  $S_1$  can be ascribed to fluctuations; one may speculate that the excess strength is due to an intermediate state in the  $^{56}\text{Mn}$  compound system at some 50 keV above the neutron binding energy with a width of perhaps 20 keV. We prefer the lower value of  $S_1 = (0.36_{-0.04}^{+0.05}) \times 10^{-4} eV^{1/2}$ , since this spans the neutron energy region up to the maximum energy of 112 keV providing a better statistical sample and thus smaller statistical uncertainty in the value of  $S_1$ . In addition the possible contribution from weak  $s$ -wave resonances at higher energy would make a lesser change in the strength function due to the larger value of  $kR$ . This value of  $S_1$  is consistent with values for other neighboring nuclei, and is also consistent with optical model calculations for spherical nuclei in this mass region using the model parameters derived by Garg.<sup>1</sup>

For resonances which are designated as  $d$  wave we estimate a value for  $S_2 = 1.0 \times 10^{-4} eV^{-1/2}$  which is smaller than expected in this mass region. This is of course an experimental shortcoming, since we have detected at most 18  $d$ -wave levels constituting only about 17% of the levels although a larger percentage of the  $d$ -wave strength.

#### $p$ -wave level spacing

After correcting for the presence of  $d$ -wave levels one obtains a revised value for  $D_{l=1} = (1.32 \pm 0.11) \times 10^{-4} \text{ keV}$  and a ratio for  $D(l=0)/D(l=1)$  ( $1.70_{-0.30}^{+0.36}$ ) which is in good agreement with the prediction of the level density formula.

#### Uncertainty in resonance energies

The uncertainty in the resonance energies is estimated as  $\pm E/1200$ , based on the assumption that the resonance peaks could be determined to about one-half the resolution width at all energies. For a comparison of resonance energies determined here with the values from total cross section measurements, it should be noted that for broad  $s$ -wave resonances, the energies quoted by Garg<sup>1</sup> are  $R$ -matrix energy eigenvalues which do not necessarily coincide with resonance peak energies. The agreement is very good between the two sets of energy values obtained from widely different experimental measurements.

#### Radiation width distribution

Some 47  $s$ -wave radiation widths ( $\Gamma_\gamma$ ) corrected for neutron scattered sensitivity were measured up to 112 keV. The mean values for the radiation widths for  $J=2$ ,  $J=3$ , and  $J=2,3$  are as follows,

$$\langle \Gamma_\gamma \rangle_{J=2} = 710 \pm 150 \text{ meV},$$

$$\langle \Gamma_\gamma \rangle_{J=3} = 790 \pm 160 \text{ meV},$$

$$\langle \Gamma_\gamma \rangle_{J=2,3} = 750 \pm 150 \text{ meV}.$$

For  $p$ -wave resonances only 28 radiation widths were measured directly giving a mean value of  $\langle \Gamma_\gamma \rangle_{l=1} = 400 \pm 100 \text{ meV}$ . The above difference between  $\langle \Gamma_\gamma \rangle_{l=0}$  and  $\langle \Gamma_\gamma \rangle_{l=1}$  appears only modestly significant in a statistical sense. However, since most  $p$ -wave resonances have narrow widths (much less than our instrumental resolution), we are able to measure directly  $\Gamma_\gamma$ 's for only the strongest resonances and thus obtain an upper limit for  $\langle \Gamma_\gamma \rangle_{l=1}$ . From the area under the resonance only the kernel,  $g\Gamma_n\Gamma_\gamma/(\Gamma_n + \Gamma_\gamma)$  can be evaluated.  $\Gamma_n$  values for most  $p$ -wave resonances are not known from transmission work, so that values of  $\Gamma_\gamma$  cannot be computed from these measurements. In some cases at low energies we could determine both  $\Gamma_n$  and  $\Gamma_\gamma$  from the capture data, assuming an average value of  $g=0.5$ . A value of  $\Gamma_\gamma \approx 300 \text{ meV}$  was then estimated for the narrow resonances up to 32 keV. Since our least-squares analysis gave good fits for independent values of  $\Gamma_\gamma$  ( $371 \pm 31$  and  $361 \pm 32 \text{ meV}$  for resonances at 33.32 and 36.54 keV, respectively), we have assumed a value of  $\Gamma_\gamma = 400 \text{ meV}$  for most narrow resonances above 32 keV. A few values of  $\Gamma_\gamma \approx 500 \text{ meV}$  were used to determine  $g\Gamma_n$  values. Values of  $g\Gamma_n$  so estimated will have an added uncertainty associated with the fluctuation in the assumed  $g\Gamma_n$  values.

#### Correlations between reduced neutron widths and the radiation widths

The presence of a significant correlation between  $\Gamma_n$  and  $\Gamma_\gamma$  has been observed by Block *et al.*<sup>14</sup> and Beer *et al.*<sup>15</sup> for even-even nuclei in the mass region of the  $3S$  strength function maximum. The presence of this correlation is, however, not consistent with the Bohr postulates for resonance phenomena, where the decay of the compound nucleus is considered to take place according to statistical theory. Similarly, from the study of thermal neutron capture spectroscopy, the correlation between  $(n,\gamma)$  partial widths to a given final state and spectroscopic factors of nucleon transfers in  $(d,p)$  reactions to the same final state, have been observed by Kinsey *et al.*<sup>16</sup> and Groshev *et al.*<sup>17</sup> This latter effect had prompted theorists to investigate the mechanism for radiative capture. For example Lane and Lynn<sup>18</sup> have considered the capture mechanism in terms of three components, i.e., (1) compound nucleus formation according to Bohr's postulates, (2) direct or potential capture, (3) channel or valency capture. Moreover Lane<sup>19</sup> has emphasized that any significant positive correlation between partial widths

of different channels (e.g.,  $\Gamma_n$  and  $\Gamma_{\gamma i}$ ) can arise from nonstatistical effects in the radiative process. Large correlations between the above quantities could either arise from the existence of a simpler state (such as a doorway state of the proper  $J^\pi$ ) near the neutron binding energy, or it could arise if the decay process followed a direct nucleon transfer, i.e., valency capture. It would appear that a significant correlation between neutron widths and radiation widths is possible if the radiative decay process is dominated by few transitions, presumably to simple low lying states.

The (linear) correlation  $\rho$  between  $N$  pairs of quantities such as  $\Gamma_n^0$  and  $\Gamma_{\gamma}$  from a bivariate population is defined as

$$\rho(\Gamma_n^0, \Gamma_{\gamma}) = \frac{\sum_{i=1}^N (\Gamma_{ni}^0 - \bar{\Gamma}_n^0)(\Gamma_{\gamma i} - \bar{\Gamma}_{\gamma})}{\left[ \sum_{i=1}^N (\Gamma_{ni}^0 - \bar{\Gamma}_n^0)^2 \sum_{i=1}^N (\Gamma_{\gamma i} - \bar{\Gamma}_{\gamma})^2 \right]^{1/2}},$$

where  $\bar{\Gamma}_n^0$  and  $\bar{\Gamma}_{\gamma}$  are the mean values. This coefficient measures the degree of correlation between the two variables  $\Gamma_{\gamma i}$  and  $\Gamma_{ni}^0$ . The values of  $\rho$  can vary from +1 to -1. A correlation of  $\rho = +1$  or  $-1$  signifies complete linear dependence and  $\rho = 0$  implies that the two widths are completely independent of each other.

We have investigated the correlation between the  $s$ -wave reduced neutron widths from transmission measurements<sup>1</sup> and the radiation widths for the same resonances as evaluated in the present measurements. We have obtained the following results:  $\rho_{J=3} = (0.82 \pm 0.20)$ ,  $\rho_{J=2} = (0.53 \pm 0.19)$ ,  $\rho_{J=2,3} = (0.64 \pm 0.14)$ . The uncertainty in the value of the correlation coefficient can be obtained from the following expression<sup>19</sup>:

$$\Delta\rho^2 = \frac{\sum_{i=1}^N \Delta\Gamma_{\gamma}^2 (\Gamma_{ni}^0 - \bar{\Gamma}_n^0)^2 + \sum_{i=1}^N (\Delta\Gamma_{ni}^0)^2 (\Gamma_{\gamma i} - \bar{\Gamma}_{\gamma})^2}{\sum_{i=1}^N (\Gamma_{ni}^0 - \bar{\Gamma}_n^0)^2 \sum_{i=1}^N (\Gamma_{\gamma i} - \bar{\Gamma}_{\gamma})^2}.$$

TABLE III. Average capture cross sections for different neutron energy intervals.

Energy range (keV)	Average cross section (mb)	Rigoleur <i>et al.</i> (Ref. 4) (mb)
3-6	81.3	
6-9	186.6	
9-12	67.1	
12-15	27.7	
15-20	43.6	57.05
20-30	44.6	40.97
30-40	44.7	27.43
40-50	28.2	19.58
50-60	26.0	20.41
60-80	21.5	20.19
80-100	16.3	17.65
100-120	14.3	12.64
120-140	15.2	11.53
140-160	8.3	
160-180	8.6	
180-200	8.3	
200-220	6.5	
220-240	6.3	8.56
240-260	5.6	7.65
260-280	5.6	7.70
280-300	6.6	6.50
300-320	5.8	4.66
320-340	5.7	4.28
340-360	5.8	5.36
360-380	4.3	
380-400	5.1	4.54
400-420	5.9	4.11
420-440	5.0	3.30
440-460	5.6	2.77
460-480	5.6	3.35
480-500	4.6	3.25
500-550	4.2	
550-600	4.8	
600-650	3.8	
650-700	4.3	

Further, it is necessary to determine if the observed correlation is significantly different from zero. In a finite sample of two variables, a positive correlation coefficient can occur purely by chance, and it is thus necessary to determine the level of significance. To do this, a random sample of pairs of reduced neutron widths with a Porter-Thomas distribution and radiation widths consisting of about 20 channels were evaluated using a Monte Carlo program. The calculation gave a probability of 0.001 that a random distribution of these pairs would produce a correlation coefficient as large as that observed, i.e., the observed correlation is significant at the 99.9% confidence level.

Since the value of correlation between  $\Gamma_n^0$  and  $\Gamma_\gamma$  depends upon the values of  $\Gamma_\gamma$  which requires correction for neutron sensitivity factor ( $k$ ), it was considered essential to reevaluate this quantity for the case where the  $k$  values were systematically increased by 30%. A value of  $\rho = (0.42 \pm 0.14)$  was obtained for the contribution of resonances of both spins. This value though smaller than that obtained for values of  $k$  given in Table I, is found again to be statistically significant at the 99.6% level of confidence. Hence, the present results do appear to confirm the earlier findings of Block *et al.*<sup>14</sup>

#### Average capture cross section

Analysis of the current data above 112 keV is seriously compromised due to limitations in instrumental resolution. However, the average value of the capture cross sections can be obtained over various energy intervals. We have calculated the average capture cross section values in the energy range of 3 to 700 keV for varying energy intervals as given in Table III. These values of

the average capture cross section show wide fluctuations depending upon the presence of resonances and size of the interval chosen, particularly at the lower energies. The average capture cross section value can also be calculated theoretically if the values of the strength functions ( $S_l$ ), mean radiation widths, and level spacings are known for each value of  $l$ , and if competition from inelastic channels is not present (or has been measured). In Mn the first inelastic channel opens up at 126 keV and the second excited state is at 926 keV. The agreement of our average data with the calculations is not good at higher energies due largely to the inadequacies of our treatment which uses a single value of  $\bar{\Gamma}_\gamma$  in evaluating  $(\bar{\Gamma}_\gamma / \langle D \rangle)$ , whereas we observe different values of  $\bar{\Gamma}_\gamma$  and  $\langle D \rangle$  for different  $l$  values.

#### CONCLUSIONS

These high resolution capture cross section measurements in manganese permit evaluation of the  $p$ -wave strength function. It is found to be consistent both with values found for neighboring nuclei and with optical model calculations using the parameters of Garg.<sup>1</sup> We have extracted a value for the mean spacing of  $p$ -wave resonances as well as mean values of radiation widths for  $p$ - and  $s$ -wave resonances. A significant correlation between the radiation widths and reduced neutron widths of  $s$ -wave resonances has been observed which confirms earlier findings of Block *et al.*<sup>14</sup> and suggests the presence of a nonstatistical radiative decay process in this nucleus.

We would like to thank Jack Craven and Judd Bernard for their help in computer programming and Dr. Ron Winters for many helpful discussions. This research was supported in part by the U.S.D.O.E.

<sup>1</sup>J. B. Garg, Nucl. Sci. Eng. 65, 76 (1978).

<sup>2</sup>J. Morgenstern *et al.*, Nucl. Phys. A102, 602 (1967).

<sup>3</sup>G. Rohr and E. Friedland, Nucl. Phys. A104, 1 (1967).

<sup>4</sup>C. LeRigoleur, A. Arnaud, and J. Taste, Report No. CEA-R-4788, Saclay, France, 1976 (unpublished).

<sup>5</sup>R. L. Macklin and B. J. Allen, Nucl. Instrum. Methods 91, 565 (1971).

<sup>6</sup>B. J. Allen and R. L. Macklin, Phys. Rev. C 3, 1737 (1971).

<sup>7</sup>B. J. Allen, R. L. Macklin, R. R. Winters, and C. Y. Fu, Phys. Rev. C 8, 1504 (1973).

<sup>8</sup>R. L. Macklin, Nucl. Sci. Eng. 59, 12 (1976).

<sup>9</sup>F. H. Frohner, "TACASI," Report No. GA-6906 General Atomic, 1966 (unpublished).

<sup>10</sup>J. B. Garg, J. Rainwater, and W. W. Havens, Jr.,

Report No. CR1860, 1964 (unpublished); J. B. Garg, Nucl. Sci. Eng. 65, 76 (1978).

<sup>11</sup>T. E. Stephenson and S. Pearlstein, Nucl. Sci. Eng. 32, 377 (1968).

<sup>12</sup>S. F. Mughabghab *et al.* private communication (unpublished).

<sup>13</sup>C. E. Porter and R. G. Thomas, Phys. Rev. 104, 483 (1956).

<sup>14</sup>R. C. Block, R. G. Stieglitz, and R. W. Hockenbury, Proceedings of the Conference on Neutron Cross Sections and Technology, Lowell, 1976, Report No. CONF-760715 PI (unpublished), p. 889.

<sup>15</sup>H. Beer and R. R. Spencer, Nucl. Phys. A240, 29 (1975).

<sup>16</sup>B. B. Kinsey, G. A. Bartholomew, and W. H. Walker,

- Phys. Rev. 83, 519 (1951).
- <sup>17</sup>L. V. Groshev, A. M. Demidov, U. N. Lutsenko, and V. J. Pelenkov, *Proceedings of the International Conference on the Peaceful Uses of Atomic Energy, Geneva* (United Nations, New York, 1958), Vol. 15, p. 138.
- <sup>18</sup>A. M. Lane and J. E. Lynn, Nucl. Phys. 17, 1563 (1960).
- <sup>19</sup>A. M. Lane, Am. Phys. (N.Y.) 63, 171 (1971).